Liquid Crystals

Electrodeposition of Silver Particles and Gold Nanoparticles from Ionic Liquid-Crystal Precursors**

*William Dobbs, Jean-Moïse Suisse, Laurent Douce,* and Richard Welter*

Dedicated to Stéphane Bellemin-Laponnaz

The convergence of two distinct fields of ionic liquid chemistry, those of imidazolium salts and liquid crystals, could lead to a vast range of new materials.[1] Uniting the properties of imidazolium derivatives, which have low melting points, low volatility, nonflammability, high chemical and radiochemical stability, tunable conductivity, and wide electrochemical windows, with those of liquid crystals, which have many forms of labile macroscopic ordering, raises fascinating prospects.[1,2] A particular challenge is the synthesis of nanoparticles of controllable form for applications in electronics, catalysis, and materials science.[3] Solvents based on imidazolium and pyridinium salts have been successfully used to prepare and stabilize gold nanoparticles or nanorods, for example, but the literature concerning mesomorphic pyridinium and imidazolium salts incorporating metalloanions is very limited.[4–8] A significant recent report is the use of an ionic liquid crystal, *N*-dodecylpyridinium tetrachlorocuprate(II), mixed with the hydrophobic reducing agent 6-*O*-palmitoyl ascorbic acid, as a template to synthesize copper(I) chloride nanoplatelets.[9]

We now present a strategy for a more versatile exploitation of liquid-crystal template effects, which is illustrated by the electrolysis of imidazolium liquid crystals containing dicyanoargentate(I) and dicyanoaurate(I) anions to produce silver and gold nanoparticles. The key to this approach is the coupling of the self-organization of the imidazolium metallate

[*] W. Dobbs, J.-M. Suisse, Dr. L. Douce
Institut de Physique et Chimie des Matériaux de Strasbourg
Groupe des Matériaux Organiques
UMR 7504, CNRS-Université Louis Pasteur
BP 43, 23 rue du Loess, 67034 Strasbourg Cedex 2 (France)
Fax: (+33) 388-107-246
E-mail: Laurent.Douce@ipcms.u-strasbg.fr
Prof. R. Welter
Laboratoire DECOMET
UMR 7177-LC003, CNRS-Université Louis Pasteur
4 rue Blaise Pascal, 67000 Strasbourg Cedex (France)

to the use of electrochemical reduction, the latter providing the means to control the particle size and form of the electrodeposited metals by variation of parameters such as the potential and the current density.

Many mesomorphic imidazolium salts can be readily prepared by simple metathesis reactions involving precipitation from aqueous solutions containing the appropriate anions. In investigating this chemistry, we sought to use anions incorporating transition metals to endow the products with properties such as redox activity and variable conductivity. Thus, we have synthesized dicyanoargentate(I) (**1**) and dicyanoaurate(I) (**2**) derivatives of 3-(4-dodecyloxybenzyl)-1-methyl-1*H*-imidazolium in good yield (over 80%) from the bromide starting material (Scheme 1).[10] Both complex salts are highly insoluble in water and are isolated in pure form by simply washing the reaction precipitates with water.
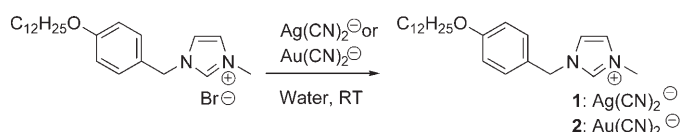
Scheme 1. Precipitation of **1** and **2** from water.

Compounds **1** and **2** were characterized by ^{1}H NMR, ^{13}C{^{1}H} NMR, and FT-IR spectroscopy, and elemental analysis. Distinctive signals assigned to the CH group at the 2-position of the imidazolium ring appear in the ^{1}H NMR spectra of **1** and **2** at $\delta = 9.05$ and 8.77 ppm, and in their ^{13}C{^{1}H} NMR spectra at $\delta = 136.14$ and 135.50 ppm, respectively. The IR spectra of **1** and **2** show typical cyanometallate vibrations at $\tilde{\nu}(CN) = 2131$ and 2140 cm^{-1}, respectively.[11]

Single crystals of **1** and **2** were obtained by the slow diffusion of ether into dichloromethane solutions, and the structures of the compounds were determined by X-ray diffraction (see Supporting Information). As the crystal structures of **1** and **2** are isotypic, we only describe that of **2**, which is shown in Figure 1. In the cation, the *n*-alkyl chains and the phenyl groups are approximately orthogonal (87(1)°) to the plane of the imidazolium ring.
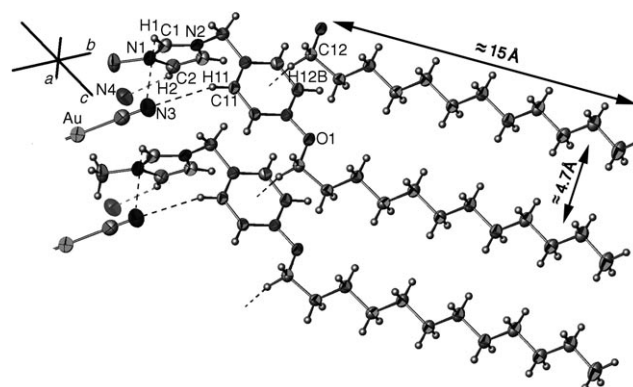

Figure 1. ORTEP representation of part of the crystal structure of **2**. Dashed lines indicate nonclassical hydrogen bonds. Thermal ellipsoids enclose 50% of the electron density.

The packing in the crystal structure can be described as a pseudo-lamellar system with a stacking direction along the *c* axis (Figure 2). Nonclassical hydrogen bonds (N4···H2−C2, N3···H1−C1, and N3···H11−C11) associate the $[Au(CN)_2]^-$
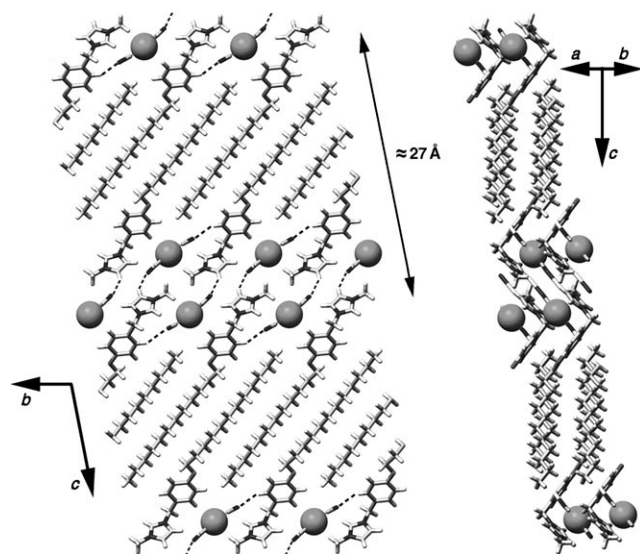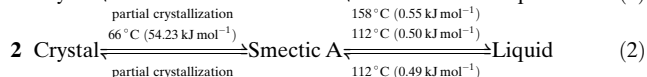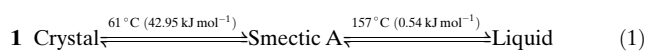

Figure 2. Two views of the crystal structure of **2**. Dashed lines indicate nonclassical hydrogen bonds. Au spheres; C, H, N, O rods.

anion with the rigid imidazolium and phenyl rings of the cation (Figure 1). Moreover, a C−H···π interaction occurs between C12−H12B and the phenyl ring (the distance between H12B and the centroid of the ring is 2.76 Å). The rigid phenyl and imidazolium rings form a unit of approximately 7 Å in length. These units, together with the $[Au(CN)_2]^-$ anions, comprise layers that are completely segregated by the flexible chains of approximately 15 Å in length. The layers are stacked along the *c* axis at a repeat distance of approximately 27 Å (Figure 2).

The formation of true crystals of **1** and **2** at ambient temperatures is not unexpected, since the balance of factors influencing crystallinity and mesomorphism is subtle. The amphiphilic character of these materials leads, however, to the expectation that mesomorphism should be exhibited at higher temperatures.

The mesomorphic behavior and phase-transition temperatures of **1** and **2** were characterized by polarizing optical microscopy (POM), differential scanning calorimetry (DSC), and powder X-ray diffraction (XRD). The DSC thermograms registered upon heating and cooling reveal for both **1** and **2** the presence of two sharp peaks indicative of reversible first-order phase transitions. The first peak (at low temperature with a large enthalpy change) is related to the appearance of a liquid-crystal phase, while the second peak is due to its melting into an isotropic liquid. These observations can be summarized by Equations (1) and (2), in which the phase-transition temperatures and enthalpy changes are indicated.

$$\textbf{1} \quad \text{Crystal} \underset{\substack{\longleftarrow \\ \text{partial crystallization}}}{\overset{\substack{61\,°C\ (42.95\ \text{kJ mol}^{-1}) \\ \longrightarrow}}{}} \text{Smectic A} \underset{\substack{\longleftarrow \\ 158\,°C\ (0.55\ \text{kJ mol}^{-1})}}{\overset{\substack{157\,°C\ (0.54\ \text{kJ mol}^{-1}) \\ \longrightarrow}}{}} \text{Liquid} \quad (1)$$

$$\textbf{2} \quad \text{Crystal} \underset{\substack{\longleftarrow \\ \text{partial crystallization}}}{\overset{\substack{66\,°C\ (54.23\ \text{kJ mol}^{-1}) \\ \longrightarrow}}{}} \text{Smectic A} \underset{\substack{\longleftarrow \\ 112\,°C\ (0.49\ \text{kJ mol}^{-1})}}{\overset{\substack{112\,°C\ (0.50\ \text{kJ mol}^{-1}) \\ \longrightarrow}}{}} \text{Liquid} \quad (2)$$

The optical textures observed upon slow cooling from the isotropic melt show the emergence of a typical smectic-A phase: initially bâtonnets (rods) appear, and these turn into focal conic structures (Figure 3).
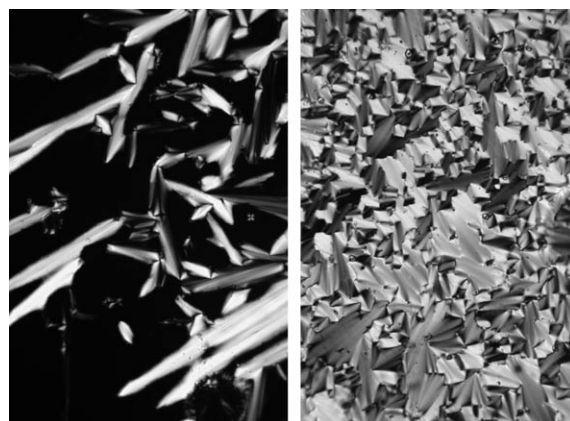

Figure 3. Polarizing optical microscope images of the smectic-A phase of **2**. Upon formation of the liquid-crystal phase, rods (left) initially appear, followed by focal conic structures (right).

The lamellar arrangement of the liquid-crystal phase was also established by XRD. Because of the high X-ray mass attenuation coefficients of gold and silver atoms, we prepared thin films of **1** and **2** between two mica slides with a 100-μm separation. The smectic-A structures produced diffraction patterns containing one sharp reflection in the small-angle region, which arises from the regular arrangement of the molecules in layers with separations of $d = 37.0$ and 36.0 Å at 100°C for **1** and **2**, respectively. A broad band at $d = 4.6$ Å in the wide-angle region of the patterns is related to the disordered (liquid-like) conformation of the alkyl chains. The diffraction patterns are consistent with a head-to-tail molecular arrangement of the cations within the layers, as observed for imidazolium salts containing PF_6^-, BF_4^-, Br^-, and SCN^- anions, in which the lamellar spacings are approximately 37 Å.[10]

To investigate the possibility of forming nanoparticles from **1** and **2** by electrodeposition, we sandwiched the compounds between two indium tin oxide (ITO) coated glass slides separated by a 100-μm spacer. The electrodeposition was conducted at constant potential for 15 minutes. In Figure 4, scanning electron micrographs (SEM) of the gold particles obtained by electrodeposition of **2** from the isotropic liquid state at 117°C (top) and from the liquid-crystal state at 111°C (bottom) are shown. The particles formed by electrodeposition from the isotropic liquid are nanodots (20–30 nm) aggregated into spheres or multiglobular shapes (100 nm). In contrast, the morphology of the nanoparticles deposited from the liquid crystal at 111°C is completely different, consisting of leaflike forms interlocked in rosettes.

Application of the same electrodeposition procedure to the isotropic liquid of the silver derivative **1** led to essentially polydisperse silver spheres at 170°C (Figure 5, top). Electrodeposition at 152°C from the mesomorphic phase of **1** led to hexagonal platelets in an amorphous silver gangue (Figure 5,
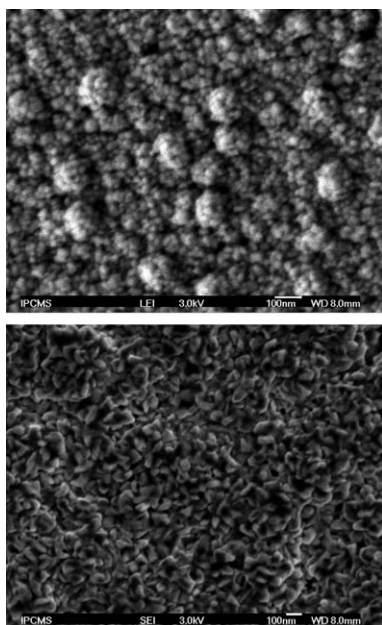
Figure 4. SEMs of spherical gold nanoparticles electrodeposited ($E = 1.78$ V) from the isotropic liquid phase of **2** (top), and of leaflike gold forms electrodeposited ($E = 2.27$ V) from the lamellar liquid-crystal phase of **2** (bottom). White scale bars: 100 nm.
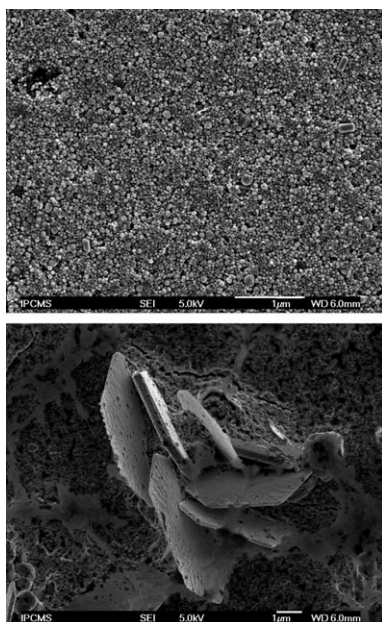

Figure 5. SEMs of spherical silver nanoparticles electrodeposited ($E = 1.21$ V) from the isotropic liquid phase of **1** (top), and of hexagonal silver platelets electrodeposited ($E = 1.70$ V) from the lamellar liquid-crystal phase of **1** (bottom). White scale bars: 1 μm.

bottom). These platelets are remarkably similar to the CuCl platelets obtained from a lamellar ionic liquid-crystal precursor.[9]

In summary, we report the full characterization of the first mesomorphic compounds based on imidazolium cyanometallates. The structures of their crystalline phases have also been determined. Work is in progress on the modification of the

structures to provide ambient-temperature mesophases and other forms of self-organization. Of particular significance is the demonstration herein that the supramolecular structure of the liquid-crystal phase can be used to influence the morphology of metal nanoparticles deposited by electrochemical reduction.

Experimental Section

1: Compound **1** was obtained by anion metathesis in water. An aqueous solution (25 mL) of potassium dicyanoargentate (467 mg, 2.35 mmol) was added to 3-(4-dodecyloxybenzyl)-1-methyl-1*H*-imidazolium bromide (1.03 g, 2.35 mmol) dissolved in water (50 mL). A precipitate of **1** formed immediately, and was collected by filtration and washed with water. Recrystallization by slow diffusion of ether into a dichloromethane solution led to a white crystalline solid, yield: 1.22 g, 92%. ^{1}H NMR (300 MHz, CDCl$_3$): $\delta = 0.89$ (t, ^3J(H,H) = 6.6 Hz, 3H, C*H*$_3$ aliphatic chain), 1.27 (br s, 16H, C*H*$_2$ aliphatic chain), 1.39–1.47 (m, 2H, C*H*$_2$ aliphatic chain), 1.76 (q, ^3J(H,H) = 6.8 Hz, 2H, OCH$_2$C*H*$_2$), 3.98 (t, ^3J(H,H) = 6.6 Hz, 2H, OC*H*$_2$), 4.03 (s, 3H, C*H*$_3$N), 5.31 (s, 2H, NC*H*$_2$Ph), 6.97 (d, ^3J(H,H) = 8.6 Hz, 2H, C*H* phenyl), 7.24–7.26 (m, 2H, NC*H* imidazolium), 7.35 (d, ^3J(H,H) = 8.6 Hz, 2H, C*H* phenyl), 9.05 ppm (s, 1H, NC*H*N imidazolium); ^{13}C NMR (75 MHz, CDCl$_3$): $\delta = 14.09$ (*C*H$_3$ aliphatic chain), 22.65, 25.99, 29.13, 29.31, 29.37, 29.54, 29.57, 29.60, 29.63, 31.88 (*C*H$_2$ aliphatic chain), 36.95 (N*C*H$_3$), 53.52 (N*C*H$_2$Ph), 67.26 (O*C*H$_2$), 115.57 (*C*H phenyl), 122.08, 123.38 (N*C*H imidazolium), 123.42 (*C* phenyl), 123.65 (N*C*H imidazolium), 130.60 (*C*H phenyl), 136.14 (N*C*HN imidazolium), 144.74 (*C*N), 160.37 ppm (*C* phenyl); IR: $\tilde{v} = $ 3154, 2915, 2846, 2131, 1515, 1255, 1248 cm^{-1}. Elemental analysis (%) calcd for C$_{25}$H$_{37}$AgN$_4$O: C 58.0, H 7.2, N 10.8; found: C 58.0, H 7.4, N 10.0.

2: The same experimental procedure was used as for **1**, with potassium dicyanoaurate (164 mg, 0.57 mmol) and 3-(4-dodecyloxy-benzyl)-1-methyl-1*H*-imidazolium bromide (250 mg, 0.57 mmol). White solid, yield: 275 mg, 80%. ^{1}H NMR (300 MHz, CDCl$_3$): $\delta = $ 0.89 (t, ^3J(H,H) = 6.6 Hz, 3H, C*H*$_3$ aliphatic chain), 1.27 (br s, 16H, C*H*$_2$ aliphatic chain), 1.39–1.47 (m, 2H, C*H*$_2$ aliphatic chain), 1.80 (q, ^3J(H,H) = 6.8, 2H, OCH$_2$C*H*$_2$), 3.98 (t, ^3J(H,H) = 6.6, 2H, OC*H*$_2$), 4.03 (s, 3H, C*H*$_3$N), 5.31 (s, 2H, NC*H*$_2$Ph), 6.97 (d, ^3J(H,H) = 8.6 Hz, 2H, C*H* phenyl), 7.24–7.26 (m, 2H, NC*H* imidazolium), 7.35 (d, ^3J(H,H) = 8.6 Hz, 2H, C*H* phenyl), 8.77 ppm (s, 1H, NC*H*N imidazolium); ^{13}C NMR (75 MHz, CDCl$_3$): $\delta = 14.11$ (*C*H$_3$ aliphatic chain), 22.67, 26.00, 29.14, 29.33, 29.38, 29.56, 29.59, 29.62, 29.65, 31.90 (*C*H$_2$ aliphatic chain), 37.05 (N*C*H$_3$), 53.70 (N*C*H$_2$Ph), 68.29 (O*C*H$_2$), 115.65 (*C*H phenyl), 122.26, 122.99 (N*C*H imidazolium), 123.74 (*C* phenyl), 130.82 (*C*H phenyl), 135.50 (N*C*HN imidazolium), 151.17 (*C*N), 160.47 ppm (*C* phenyl); IR: $\tilde{v} = 3101$, 2916, 2846, 2140, 1515, 1256, 1249 cm^{-1}. Elemental analysis (%) calcd for C$_{25}$H$_{37}$AuN$_4$O: C 49.5, H 6.15, N 9.2; found: C 49.1, H 6.3, N 8.9.

DSC: Perkin Elmer Q1000, heating/cooling rate of 2°C min^{-1}. Polarizing optical microscope: Leitz Orthoplan, Mettler FP82 hot stage. Powder XRD: Cu$_{K\alpha1}$ radiation, powder samples in Lindemann capillaries, INSTEC hot stage, image plate. SEM: JEOL JMS 6700F with a Noran Vantage energy-dispersive X-ray spectrometer.

Single-crystal XRD: The selected crystals were mounted on a Nonius KappaCCD area-detector diffractometer (Mo$_{K\alpha}$, $\lambda = $ 0.71073 Å). Cell parameters were determined from reflections recorded in ten frames (1.0° in ϕ, 20 s). The structures were solved using direct methods (SHELXS97) and refined against F^2 (SHELXL97). All non-hydrogen atoms were refined anisotropically. Hydrogen atoms were generated according to stereochemistry and refined using a riding model. Further details of the data collections (Denzo) and structure refinements are given in the Supporting Information. **1**: colorless crystal, $0.11 \times 0.10 \times 0.09$ mm^3, C$_{25}$H$_{37}$AgN$_4$O, $M_r = 517.46$ g mol^{-1}, triclinic, space group $P\bar{1}$, $a = $

[1] H. Ohno, *Electrochemical Aspects of Ionic Liquids*, Wiley-Interscience, New York, **2005**; P. Wasserscheid, T. Welton, *Ionic Liquids in Synthesis*, Wiley-VCH, Weinheim, **2003**; J. Dupont, R. F. de Souza, P. A. Z. Suarez, *Chem. Rev.* **2002**, *102*, 3667; J. W. Goodby, G. W. Gray, H.-W. Spiess, V. Vill, D. Demus, *Handbook of Liquid Crystals*, Wiley-VCH, Weinheim, **1998**.

[2] F. Endres, *ChemPhysChem* **2002**, *3*, 144; D. Allen, G. Baston, A. E. Bradley, T. Gorman, A. Haile, I. Hamblett, J. E. Hatter, M. J. F. Healey, B. Hodgson, R. Lewin, K. V. Lovell, B. Newton, W. R. Pitner, D. W. Rooney, D. Sanders, K. R. Seddon, H. E. Sims, R. C. Thied, *Green Chem.* **2002**, *4*, 152; A. J. Arduengo III, *Acc. Chem. Res.* **1999**, *32*, 913; A. J. Arduengo, T. Bannenberg, *The Strem Chemiker* **2002**, *19*, 1.

[3] G. Cao, *Nanostructures and Nanomaterials: Synthesis, Properties and Applications*, Imperial College Press, London, **2004**; M.-C. Daniel, D. Astruc, *Chem. Rev.* **2004**, *104*, 293.

[4] K. Binnemans, *Chem. Rev.* **2005**, *105*, 4148.

[5] G. T. Wei, Z. Yang, C. Y. Lee, H-Y Yang, C. R. Wang, *J. Am. Chem. Soc.* **2004**, *126*, 5036; C. Scheeren, G. Machado, J. Dupont, P. Fichtner, S. Ribiero-Texeira, *Inorg. Chem.* **2003**, *42*, 4738.

[6] F. Neve, O. Francescangeli, A. Cripini, *Inorg. Chim. Acta* **2002**, *338*, 51; F. Neve, O. Francescangeli, A. Cripini, J. Charmant, *Chem. Mater.* **2001**, *13*, 2032; F. Neve, S. Armentano, A. Cripini, O. Francescangeli, *Chem. Mater.* **1998**, *10*, 1904.

[7] C. K. Lee, H. H. Peng, I. J. B. Lee, *Chem. Mater.* **2004**, *16*, 530; C. Hardacare, J. D. Holbrey, P. B. McCornac, S. E. J. McMath, M. Nieuwenhuyzen, K. R. Seddon, *J. Mater. Chem.* **2001**, *11*, 346; E. R. Schreiter, J. E. Stevens, M. F. Ortwerth, G. Freeman, *Inorg. Chem.* **1999**, *38*, 3935; C. J. Bowlas, D. W. Bruce, K. R. Seddon, *Chem. Commun.* **1996**, 1652.

[8] Y. Yoshida, K. Muroi, A. Otsuka, G. Saito, M. Takahashi, T. Yoko, *Inorg. Chem.* **2004**, *43*, 1458.

[9] A. Taubert, P. Steiner, A. Mantion, *J. Phys. Chem. B* **2005**, *109*, 15542; A. Taubert, *Acta Chim. Slov.* **2005**, *52*, 183; A. Taubert, *Angew. Chem.* **2004**, *116*, 5494; *Angew. Chem. Int. Ed.* **2004**, *43*, 5380.

[10] W. Dobbs, L. Douce, L. Allouche, A. Louati, F. Malbosc, R. Welter, *New J. Chem.* **2006**, *30*, 528.

[11] K. Nakamoto, *Infrared and Raman Spectra of Inorganic and Coordination Compounds*, 4th ed., Wiley-Interscience, New York, **1986**.